HOKKAIDO UNIVERSITY

Title	Bright single-photon source based on an InAs quantum dot in a silver-embedded nanocone structure
Author(s)	Liu, X.; Asano, T.; Odashima, S.; Nakajima, H.; Kumano, H.; Suemune, I.
Citation	Applied Physics Letters, 2013(102), 131114 https://doi.org/10.1063/1.4801334
Issue Date	2013-04-05
Doc URL	http://hdl.handle.net/2115/54792
Rights	Copyright 2013 American Institute of Physics. This article may be downloaded for personal use only. Any other use requires prior permission of the author and the American Institute of Physics. The following article appeared in Appl. Phys. Lett. 102, 131114(2013) and may be found at http://apl.aip.org/resource/1/applab/v102/i13/p131114_s1.
Type	article
File Information	ApplPhysLett_102_131114.pdf

Instructions for use

Hokkaido University Collection of Scholarly and Academic Papers : HUSCAP

Bright single-photon source based on an InAs quantum dot in a silver-embedded nanocone structure

X. Liu,[1,a)] T. Asano,[1] S. Odashima,[1] H. Nakajima,[1,2] H. Kumano,[1] and I. Suemune[1]
[1]*Research Institute for Electronic Science, Hokkaido University, Sapporo 001-0021, Japan*
[2]*Research Fellow of the Japan Society for the Promotion of Science, Tokyo 102-8472, Japan*

(Received 2 February 2013; accepted 25 March 2013; published online 5 April 2013)

High photon-extraction efficiency is strongly required for a practical single-photon source. We succeed in fabricating metal (sliver)-embedded nanocone structure incorporating an InAs quantum dot. Efficient photon emission of ~200 000 photons per second is detected and single-photon emission is demonstrated using autocorrelation measurements. The photon-extraction efficiency as high as 24.6% is obtained from the structure. © *2013 AIP Publishing LLC*. [http://dx.doi.org/10.1063/1.4801334]

Within the past decade, much attention has been devoted to the development of single-photon sources for future applications in quantum information processing and quantum communications based on a wide variety of systems, such as single atoms, molecules, and color centers in diamonds.[1–3] Among these systems, single quantum dots (QDs) are potential candidates owing to their discrete levels, which offer high emission rates, narrow spectral line widths, and wide tunability of emission wavelengths.[4–9] Significant progress has been made to achieve efficient single-photon sources. One of the key issues is to enhance photon-extraction efficiency, which is defined as the collection efficiency of photons emitted from a QD into the first lens in an experimental optical setup. Efficient single-photon emission has been demonstrated from single QDs in distributed Bragg reflector (DBR) microcavities with pillar structures[4,5] and inner lateral confinement,[6] photonic nanowires,[7,8] trumpet structures,[9] horn structures,[10] and so on. Coupling of photon emission from QDs to metallic nanoantennas,[11] confined plasmon modes,[12] as well as photonic waveguides[13] was also proposed. Although photonic nanowires and microcavity pillars exhibited high photon-extraction efficiencies, mechanical stability related to their high aspect ratio and their stability to couple to outer photon collection optics remain as challenging issues.

Recently, we have introduced a metal-embedded GaAs pillar structure containing single InAs QDs.[14,15] This structure is completely embedded in metal and is fundamentally flat and mechanically stable. Direct contact of this kind of photon sources to a single-mode fiber will provide a fiber-based photon source with long-term stability.[16] With this metal-embedded pillar structure, we have observed the photon-extraction efficiency of ~8% (efficiency collected by the first lens with the numerical aperture (NA) of 0.42).[14] In this case, GaAs substrates were removed by mechanical cleavage during the metal-embedding process, and hard metals were necessary for the sample preparation. Therefore, titanium (Ti) and/or niobium (Nb) hard metals were selected for the embedding metals in these samples.[15,17] However, optical reflectivity of these hard metals is generally low, and it is a drawback for efficient photon extraction. Silver (Ag) is known to have high optical reflectivity in the near-infrared spectral region although the Vickers hardness of Ag is ~1/4 and ~1/5 of that of Ti and Nb, respectively. In this paper, we report on the preparation of Ag-embedded QD structure via the substrate removal with reactive ion etching (RIE). A nanocone semiconductor structure with truncated apex was embedded in Ag for high photon extraction.

InAs QDs were grown on a GaAs (100) substrate by metal organic molecular beam epitaxy (MOMBE)[18] and then capped with a GaAs layer with the thickness of 50 nm. The QD density was estimated to be $\sim 8 \times 10^9\,\mathrm{cm}^{-2}$. For the fabrication of a tailored nanocone structure, electron beam lithography (EBL) and RIE processes were performed. The InAs QD sample surface was covered with a SiO_2 layer for better adhesion of hydrogen silsesquioxane (HSQ) resist to the GaAs surface. After EBL, the resist patterns were transferred to the SiO_2 layer with RIE. The GaAs-based semiconductor was etched with inductive coupled plasma (ICP) RIE employing chlorine (Cl_2) and argon (Ar) mixture gas. This resulted in the nanocone with the truncated apex (mesa structure) as typically shown in Fig. 1(a). The height is ~500 nm and the sidewall taper angle was 23.5° on average. The structure shown in Fig. 1(a) was prepared with the computer-aided design (CAD) mask diameter of 1000 nm and the top diameter is 760 nm. Therefore, 120-nm side etching from the SiO_2 mask periphery contributed to the nanocone formation, but the additional expansion of the bottom diameter by ~200 nm from the CAD diameter is also included. When the SiO_2 mask diameter is 240 nm, real nanocone is formed (not shown). The diameter of the QD plane in Fig. 1(a) is ~800 nm and the number of the InAs QDs included is ~40, and the QD numbers are reduced for the reduced diameter. Such a tailored structure was then deposited with a 60-nm-thick SiO_2 layer employing plasma-enhanced chemical-vapor deposition (PECVD) and then evaporated with a ~3-μm-thick Ag film. After the Ag surface is glued to a supporting substrate, the GaAs substrate was thinned up to ~30 μm thick with mechanical polishing and sequentially etched with ICP-RIE. This resulted in the Ag-embedded nanocone structure as shown in Fig. 1(b). The buried structure is schematically shown in Fig. 1(c).

Figure 2(a) shows the micro-photoluminescence (PL) spectrum of an InAs QD in the Ag-embedded nanocone

a)Electronic mail: liuxm@es.hokudai.ac.jp

 © 2013 AIP Publishing LLC

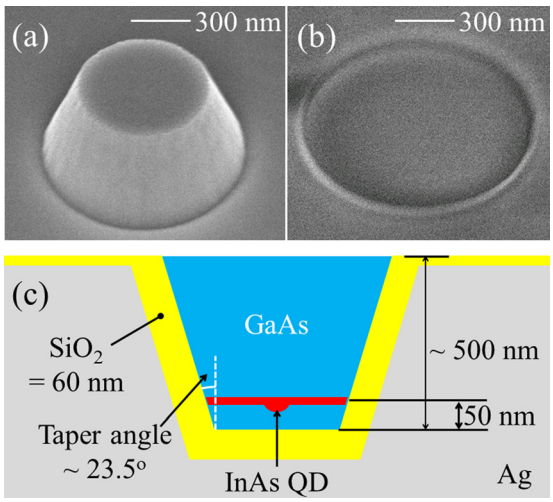

FIG. 1. (a) Side-view SEM image of an as-etched nanocone structure. (b) Top-view SEM image of the Ag-embedded nanocone structure with removed substrate. (c) Schematic of the Ag-embedded nanocone structure with a thin SiO_2 insulator layer between the Ag and the semiconductor part and an InAs QD located ~50 nm above the SiO_2.

structure fabricated with the CAD pattern diameter of 900 nm. The measurement was carried out at 4 K under the CW excitation at a wavelength of 633 nm. The PL spectrum was obtained by directing the emission into a 50 cm double grating spectrometer equipped with a liquid-nitrogen-cooled InGaAs photodiode array detector. The measured PL spectrum exhibits a sharp emission line originating from the negatively charged exciton (X^-) at 945.9 nm with a full width at half maximum (FWHM) of 152 μeV. The smaller peak at 944.1 nm is the neutral exciton (X^0) emission. The assignment of the above lines was supported by a series of measurements such as excitation power dependences and polarization-selective PL measurements. Time-resolved measurement was performed on the X^- peak by use of superconducting single-photon detectors (SSPDs) with fast response and the result is shown in Fig. 2(b). The X^- peak was spectrally selected by a tunable band-pass filter (BPF) with a FWHM of 0.5 nm and then coupled into a single-mode fiber with a microscope objective. The coupled emission signal was directed into one SSPD and the excitation pulse signal was sent to another SSPD as a synchronization input. As shown in Fig. 2(b), an instrument response function (IRF) is also given by the grey area, and the rise of the curve is limited by the temporal resolution of the system. The time

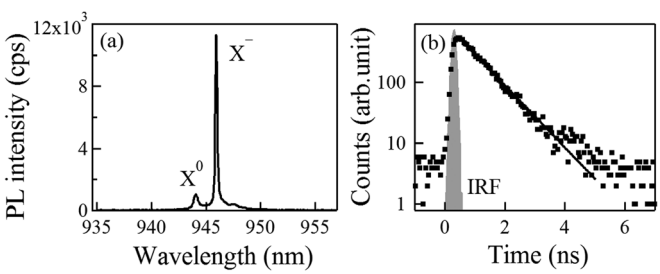

FIG. 2. (a) Micro-PL spectrum of an InAs QD in the Ag-embedded nanocone structure. The emission lines X^0 and X^- correspond to the neutral exciton emission and the negatively charged exciton emission, respectively. (b) Time-resolved signal on the X^- line. The solid line is the least-square fit to the data. The grey area corresponds to the IRF.

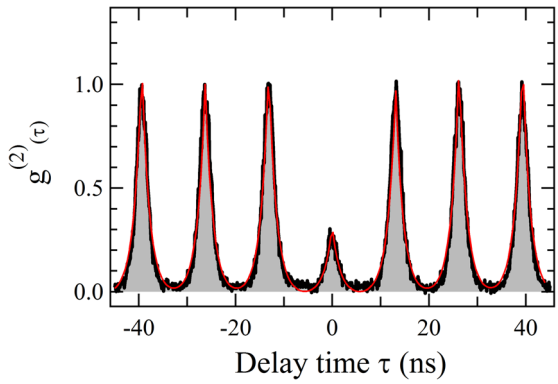

FIG. 3. Second-order correlation function $g^{(2)}(\tau)$ for the X^- line excited above saturation (1.5 μW). The solid curve in red is the least-square fit to the data.

decay behavior is fitted with a single exponential function, showing that the lifetime of the X^- line is 0.85 ns.

In order to confirm the single-photon emission property of the X^- line from a single InAs QD, we measured the second-order correlation function $g^{(2)}(\tau)$ with a Hanbury-Brown and Twiss (HBT) setup[19] under pulsed optical excitation at a wavelength of 800 nm and with a repetition rate of 76.2 MHz. The excitation pulse width was ~5 ps. The selected emission photons through the BPF were divided by a beam splitter with a 50:50 ratio and then sent into two single-photon counting modules (SPCMs). In order to compensate the electric delay of the detection system and obtain the information at the negative time delay, an optical delay of ~75 ns was inserted. Figure 3 shows the measured second-order correlation function of the X^- line as a function of the delay time τ of the two detection events. The excitation power of 1.5 μW is above the saturation level of the QD emission. The measured $g^{(2)}(\tau)$ indicates strong suppression of multi-photon emission at zero time delay and is a signature of single-photon emission. The solid curve in red is the least-square fit to the data with the commonly accepted formula.[2,15] The fitting results in $g^{(2)}(0) = 0.3$, and the anti-bunching dip below 0.5 is characteristic of a single-photon emitter (SPE). Further suppression of multi-photon emission with $g^{(2)}(0) < 0.1$ was achieved by quasi-resonant excitation with low excitation power.

We have measured the photon count rates from both as-etched and Ag-embedded nanocone structures over 20 samples. The comparison of the two structures under the saturation condition of the QD emission, which excludes the difference of the photo-excitation efficiencies, exhibited ~50 times enhancement on average with the Ag-embedding. The brightness of our SPE given above is plotted in Fig. 4, which shows the integrated photon count rate of the X^- emission. At saturation, the integrated count rate was measured to be 196 300 counts per second (cps). It is 8 times higher than our previously reported SPE.[14] The net single-photon detection rate after compensating the contribution of multi-photon emission[4] is $196\,300 \times [1 - g^{(2)}(0)]^{1/2} = 164\,200$ cps. For the estimation of the photon-extraction efficiency of the tailored structure, we experimentally estimated all the optical losses. Transmission loss including BPF, long-pass filter, short-pass filter, mirror, and objective lens was 14.3 dB. The detection efficiency of the SPCM was 0.27. From these measurements,

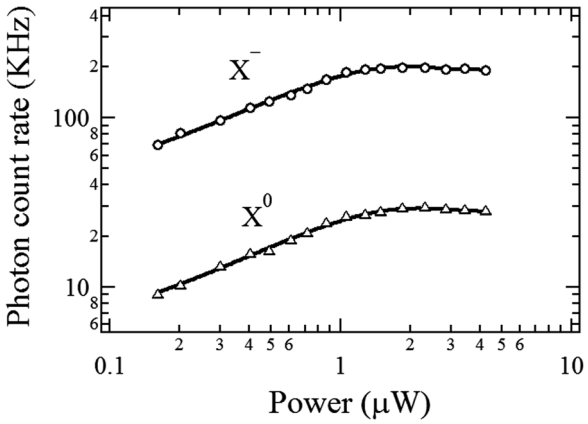

FIG. 4. The measured photon count rates of the X^- and X^0 lines as a function of excitation power. The solid curves are guides to the eye.

a single-photon flux of 16.4 MHz at the first objective lens is estimated. This estimation results in photon-extraction efficiency of 21.5% and ~0.22 photons per pulse are collected by the first objective lens. We note that the charged exciton and neutral exciton photon emission events are exclusive with each other[20] and the appearance of the X^0 peak in Fig. 2(a) indicates the underestimation of the photon-extraction efficiency.[8] From the measured photon count rates of the X^- and X^0 emission in Fig. 4, the count rates are given with the ratio of 7 to 1 above saturation. Therefore, the estimated photon-extraction efficiency is recalculated to be 24.6%.

This high photon generation rate is especially important for photon correlation measurements, since the correlation measurements depend on square of the photon generation rate. In our present measurements, we employed the first objective lens with NA of 0.42. When it is replaced with the one with NA equal to 0.8, doubled photon extraction, that is, 49% is expected.[7] We also worked on a three-dimensional finite-difference time domain (FDTD) simulation of the Ag-embedded nanocone structure. Since the calculation time is critically extended with the structure size, we worked on the simulation of a reduced-size nanocone, keeping the distance between the QD plane and the nanocone top surface the same as the measured structure. We assume the height of 300 nm and the truncated nanocone top diameter of 100 nm. With the sidewall angle of 23.5°, this results in the other plane diameter of 360 nm. A QD emitter is represented with an in-plane dipole and is assumed 50 nm apart from the nanocone plane with the 100-nm diameter and is set at the center of the QD plane. One of the important general indication of the simulation is that substantial amount of emitted photons, 67%, is absorbed by the Ag layer without the SiO_2 layer between Ag and GaAs nanocone. The optical absorption is drastically reduced with the increase of the SiO_2 layer thickness up to ~50 nm, suggesting that the coupling to the surface plasmon at the Ag/GaAs interface dominates the optical absorption loss. The efficiency to extract photons from the GaAs nanocone to the outer airside reaches as high as 98% for the thick SiO_2 layer by reducing the metal absorption. The details of the simulation will be reported elsewhere.

In conclusion, we have presented a bright single-photon source at 946 nm using a single InAs/GaAs QD in an Ag-embedded nanocone structure. We demonstrated the single-photon detection rate of 164 200 cps and the photon-extraction efficiency as high as 24.6%. The developed structure is mechanically stable and has basically flat photon extraction surface, and further study to realize coupling to a single-mode fiber for long-term stability is expected.

This work was supported in part by the Grand-in-Aid for Scientific Research (S), Grant No. 24226007, Nanotechnology Platform, and Nano-macro materials, devices and systems alliance by the Ministry of Education, Culture, Sports, Science and Technology, and SCOPE (Strategic Information and Communication R&D Promotion Programme) from the Ministry of International Affairs and Communications, Japan.

[1]M. Nothaft, S. Hohla, F. Jelezko, N. Fruhauf, J. Pflaum, and J. Wrachtrup, Nat. Commun. **3**, 628 (2012).
[2]A. Beveratos, R. Brouri, T. Gacoin, A. Villing, J.-Ph. Poizat, and P. Grangier, Phys. Rev. Lett. **89**, 187901 (2002).
[3]B. Darquié, M. P. A. Jones, J. Dingjan, J. Beugnon, S. Bergamini, Y. Sortais, G. Messin, A. Browaeys, and P. Grangier, Science **309**, 454 (2005).
[4]M. Pelton, C. Santori, J. Vučković, B. Zhang, G. S. Solomon, J. Plant, and Y. Yamamoto, Phys. Rev. Lett. **89**, 233602 (2002).
[5]O. Gazzano, S. Michaelis de Vasconcellos, C. Arnold, A. Nowak, E. Galopin, I. Sagnes, L. Lanco, A. Lemaitre, and P. Senellart, Nat. Commun. **4**, 1425 (2013).
[6]S. Strauf, N. G. Stoltz, M. T. Rakher, L. A. Coldren, P. M. Petroff, and D. Bouwmeester, Nat. Photon. **1**, 704 (2007).
[7]J. Claudon, J. Bleuse, N. S. Malik, M. Bazin, P. Jaffrennou, N. Gregersen, C. Sauvan, P. Lalanne, and J. Gerard, Nat. Photon. **4**, 174 (2010).
[8]M. E. Reimer, G. Bulgarini, N. Akopian, M. Hocevar, M. B. Bavinck, M. A. Verheijen, E. P. A. M. Bakkers, L. P. Kouwenhoven, and V. Zwiller, Nat. Commun. **3**, 737 (2012).
[9]M. Gregersen, T. R. Nielsen, J. Mork, J. Claudon, and M. Gerard, Opt. Express **18**, 21204 (2010).
[10]K. Takemoto, M. Takatsu, S. Hirose, N. Yokoyama, Y. Sakuma, T. Usuki, T. Miyazawa, and Y. Arakawa, J. Appl. Phys. **101**, 081720 (2007).
[11]A. G. Curto, G. Volpe, T. H. Taminiau, M. P. Kreuzer, R. Quidant, and N. F. van Hulst, Science **329**, 930 (2010).
[12]O. Gazzano, S. M. de Vasconcellos, K. Gauthron, C. Symonds, P. Voisin, J. Bellessa, A. Lemaitre, and P. Senellart, Appl. Phys. Lett. **100**, 232111 (2012).
[13]A. Schwagmann, S. Kalliakos, I. Farrer, J. P. Griffiths, G. A. C. Jones, D. A. Ritchie, and A. J. Shields, Appl. Phys. Lett. **99**, 261108 (2011).
[14]H. Nakajima, S. Ekuni, H. Kumano, Y. Idutsu, S. Miyamura, D. Kato, S. Ida, H. Sasakura, and I. Suemune, Phys. Status Solidi C **8**, 337 (2011).
[15]H. Nakajima, H. Kumano, H. Iijima, and I. Suemune, Appl. Phys. Lett. **101**, 161107 (2012).
[16]H. Sasakura, X. Liu, S. Odashima, H. Kumano, S. Muto, and I. Suemune, arXiv:1210.3123 [cond-mat.mes-hall].
[17]H. Kumano, H. Nakajima, S. Ekuni, Y. Idutsu, H. Sasakura, and I. Suemune, Adv. Math. Phys. **2010**, 391607 (2010).
[18]X. Zhang, S. Ganapathy, H. Kumano, K. Uesugi, and I. Suemune, J. Appl. Phys. **92**, 6813 (2002).
[19]R. H. Brown and R. Q. Twiss, Nature **177**, 27 (1956).
[20]H. Kumano, S. Kimura, M. Endo, H. Sasakura, S. Adachi, S. Muto, and I. Suemune, J. Nanoelectron. Optoelectron. **1**, 39 (2006).